An AER Contrast Retina with On-Chip Calibration

J. Costas-Santos, T. Serrano-Gotarredona, R. Serrano-Gotarredona and B. Linares-Barranco

Instituto de Microelectrónica de Sevilla (IMSE-CNM-CSIC), Dept. of Analog Design, Ed. CICA, Av. Reina Mercedes s/n, 41012 Sevilla, SPAIN. Phone: (34) 5-4239923, FAX: (34) 5-4231832, E-mail: bernabe@cnm.us.es

Abstract

We present a contrast retina microchip that provides its output as an AER (Address Event Representation) stream. Contrast is computed as the ratio between pixel photocurrent and a local average between neighboring pixels obtained with a diffusive network. This current based computation produces a large mismatch between neighboring pixels, because the currents can be as low as a few pico amperes. Consequently, a compact calibration circuitry has been included to calibrate each pixel. The paper describes the design of the pixel with its contrast computation and calibration sections. Experimental results are provided for a prototype fabricated in a standard 0.35μm CMOS process.

I. Introduction

The retina presented in this paper follows an Address-Event-Representation (AER) communication strategy. AER was first introduced by Sivilotti and colleagues [1]-[2] as a bio-inspired communication strategy for neuromorphic chips, where a large population of neurons inside a chip have to transmit their state to another population of neurons located in another chip. A common output digital bus is multiplexed and shared by all the chip neurons. Each neuron is coded with a particular address. When a particular neuron accesses the output bus, it identifies itself in the bus by writing its address on the bus. The contrast retina described in this paper transforms the continuous time contrast information computed at each pixel into a sequence of spikes. The activation level (contrast) of each neuron is coded as the time interval between two consecutive appearances of that neuron address on the output AER bus. This is known as a rate-coded information transmission strategy [3]. This way, a relevant (high-contrast) pixel uses more communication bandwidth than a less relevant one. This strategy differs from the one used by frame-based imagers that allocate equally the communication bandwidth for each pixel. Thus, they waste communication bandwidth on non or little active pixels.

The image information transmitted in the implementation presented here is the local image contrast instead of image intensity. It is known that a contrast extraction operation is done in the human retina that optimizes the information transmission through the optical nerve between the retina and the visual cortex area [4]-[5].

The main problem limiting the performance of CMOS retinae is the time-independent fixed pattern noise (FPN) or mismatch due to random variations of the electrical parameters of CMOS transistors. AER based imagers share this FPN problem. In rate-coded AER based imagers, the FPN appears as random variations of the pixel output frequency. In this paper, we propose an appropriate calibration mechanism adapted to compensate for these random frequency variations.

II. Contrast Extraction

Let us call $I_{photo}(x, y)$ the local photo current sensed by the detector at position (x, y), which is proportional to the absolute light intensity incident at that spot at a given time. Let us call $I_{avg}(x, y)$ the representation of the local average of the photo current over a certain region centered at position (x, y). We will define a measurement of the local image contrast as[1][4],

$$I_{cont}(x, y) = I_{ref}\frac{I_{avg}(x, y)}{I_{photo}(x, y)}, \quad (1)$$

where I_{ref} is a global reference current level common for all the retina pixels. The contrast is defined as the inverse ratio between the local intensity value and the background average intensity. The inverse of this relation is used by physiologists to fit responses of the retina cones [5].

Fig. 1(a) depicts the schematic of the pixel circuitry doing the contrast computation. The photo sensing device is a p^+diffusion-nwell diode with its well connected to the positive supply. The photo generated current I_{photo} is replicated twice through an NMOS-type subpico ampere current mirror formed by transistors M_1-M_4 [7]-[7]. This current mirror is able to reliably replicate input currents below the pico ampere range.

The replica of I_{photo} delivered by transistor M_2 flows into a diffusive network whose schematic is shown in Fig. 1(b) [8]-[10]. The transistors in the diffusive network operate in the subthreshold region. Each diffuser cell receives an input current $I_{photo}(x, y)$ and produces as output a current $I_{avg}(x, y)$. The operation of the diffusive network has been described in terms of 'pseudo-conductances' [9]. The current diffused through each 'pseudo-conductance' transistor ($M_2 - M_5$ in Fig. 1(b)) verifies a non-linear exponential relation in the node voltages, but an exact linear relation between the currents. As a consequence, the linear range of operation of the diffusive network extends to several orders of magnitude in the current domain. The diffusive network implements the following current diffusion equation in an exact manner:

$$I_{photo}(x, y) = I_{avg}(x, y) - \lambda_x\frac{\partial^2}{\partial x^2}I_{avg}(x, y) - \lambda_y\frac{\partial^2}{\partial y^2}I_{avg}(x, y), \quad (2)$$

where $\lambda_x = \exp((\kappa(V_j - V_o)/U_T)$, and $\lambda_y = \exp((\kappa(V_i - V_o)/U_T)$.

1. The inverse can also be defined.

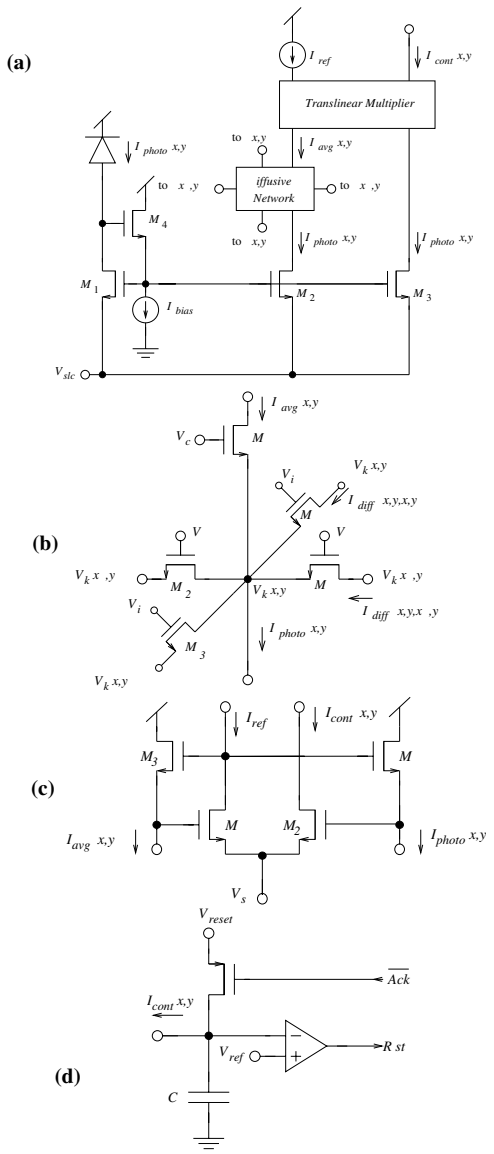

Fig. 1. (a) Pixel circuitry for contrast computation. (b) Diffusor. (c) Translinear Multiplier. (d) Subsequent integrate-and-fire.

As depicted in Fig. 1(a), the average current $I_{avg}(x, y)$ is fed to a translinear circuit. Fig. 1(c) shows the schematics of the translinear circuit. The translinear circuit also receives a copy of the local photo current $I_{photo}(x, y)$ and delivers an output current $I_{cont}(x, y)$. Transistors M_1-M_4 in Fig. 1(c) form the translinear loop, so that their currents verify the relation defined by equation (1) for contrast computation [10].

The pixel output current $I_{cont}(x, y)$ is integrated on a capacitor C as shown in Fig. 1(d). Fig. 1(d) shows a simplified schematic of the pixel integrate and fire block which performs a current-to-frequency transformation for the computed contrast. Initially, the pixel capacitor is reset to a high voltage level V_{reset}. The pixel output current $I_{cont}(x, y)$ integrated on the capacitor decreases its voltage until a certain voltage level V_{ref} is reached. When the capacitor voltage goes bellow that level, an event is sent to the periphery by activating the pixel request signal $Rqst$. Upon reception of the corresponding acknowledge from the periphery ($\overline{Ack}$ signal gets active low) the capacitor is reset to the initial level V_{ref}. Assume that the delay caused by the periphery (in the order of nanoseconds) is negligible compared to the pixel operation period (in the order of micro or mili seconds), the frequency of the events generated by a given pixel is,

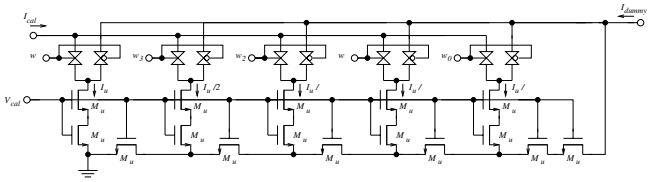

Fig. 2. Compact calibration Mini-Dac included in each pixel

$$f(x, y) = I_{cont}(x, y)\frac{V_{reset} - V_{ref}}{C}, \tag{3}$$

which is directly proportional to the pixel output current representing the pixel contrast level.

III. Calibration

As previously stated, in this AER based retina the fixed pattern noise appears as a random variation of the pixels output frequencies under uniform illumination conditions. A calibration technique is designed that equalizes all the pixel frequencies under flat illumination conditions. From eqs. (1) and (3), we can express a pixel output frequency as,

$$f(x, y) = I_{ref}\frac{V_{reset} - V_{ref}}{C}\frac{I_{avg}(x, y)}{I_{photo}(x, y)}. \tag{4}$$

Considering that all the terms in the above equation are affected by some deviation from their nominal values due to mismatching, and doing a first order Taylor expansion we can re-express the equation in the following terms,

$$\begin{aligned} f(x, y) &= I_{ref}\frac{V_{reset} - V_{ref}}{C}\frac{I_{avg}}{I_{photo}}\bigg|_{nominal} \times \\ &\times\left(1 + \frac{\Delta I_{ref}}{I_{ref}} + \frac{\Delta V}{V_{reset} - V_{ref}} - \frac{\Delta C}{C} + \frac{\Delta I_{avg}}{I_{avg}} - \frac{\Delta I_{photo}}{I_{photo}}\right) = \\ &= f|_{nominal}(1 + \Delta(x, y)) \end{aligned} \tag{5}$$

We observe that doing a first order approximation, all the error terms combine in an additive way. This is because in eq. (4) they appear either multiplying or dividing, but without additions nor subtractions. The calibration technique proposed here consists of adding a term I_{cal}/I_{ref} in equation (5) independently tunable for each pixel. This term has to compensate independently for each pixel its random total deviation $\Delta(x, y)$. A tunable current $I_{cal} = I_u\alpha(x, y)$ $(0 \le \alpha < 1)$ for each pixel is added in parallel to current I_{ref} in such a way that we equalize all the pixel firing frequencies under flat illumination conditions.

$$f(x, y) = f|_{nominal}\left(1 + \Delta(x, y) + \frac{I_u\alpha(x, y)}{I_{ref}}\right) \tag{6}$$

The generation of the tunable I_{cal} calibration current is based on the Mini-Dacs calibration technique proposed in [12]. Fig. 2 plots the schematic of the compact Mini-Dac used to generate the calibration current I_{cal} for each pixel. The mini-dac is composed of a set of unit transistors M_u, each one of size $W/L = 1\mu m/1\mu m$. Voltage V_{cal} is applied from the periphery to generate a copy of I_u in the first branch of each mini-dac. Each successive mini-dac branch generates a current which equals the current of the

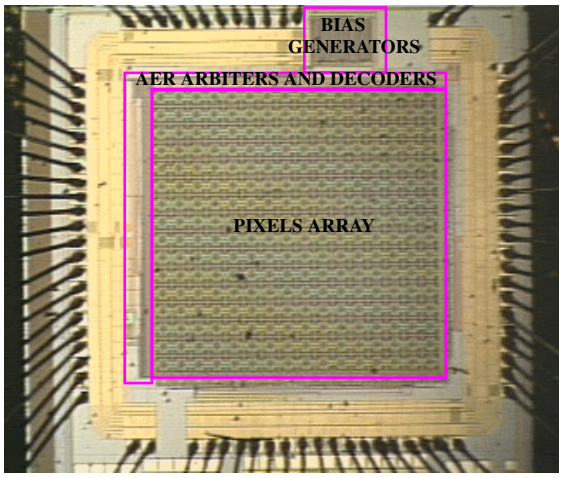

Fig. 3. Microphotograph of the 32x32 retina

preceding branch divided by 2. Each mini-dac is controlled by a 5 bit calibration word $\boldsymbol{w}_{cal} = \{w_4, w_3, w_2, w_1, w_0\}$ stored in local pixel static latches. The current generated in each branch goes to a dummy node common to all the pixels or is summed to the pixel calibration current I_{cal} depending on the state of the stored bit w_i. Thus, the calibration current can be expressed as,

$$I_{cal} = I_u \sum_{i=0}^{4} \frac{w_i}{2^{4-i}}. \qquad (7)$$

After introducing a calibration current I_{cal} in parallel with the I_{ref} current, each pixel frequency becomes a function not only of the pixel (x, y) but also of its calibration word. That is, $f(x, y, \boldsymbol{w}_{cal}(x, y))$. The calibration procedure consists of identifying for each pixel (x, y) the optimum calibration word $\boldsymbol{w}_{cal}(x, y)|_{opt}$, such that the frequency dispersion among all pixels is minimized under a condition of uniform illumination. The final reference level for which all pixel frequencies are equalized is in principle arbitrary, as long as it is within the calibration range of every pixel. We recommend to equalize for the max among all pixels, because this way average operating current increases, reducing mismatch, and improving calibration.

IV. Experimental Results

A test prototype retina of 32x32 pixels has been fabricated in the AMS-0.35µm double-poly triple-metal CMOS technology. The whole system occupies an area of $2.88mm \times 2.88mm$. Fig. 3 shows a microphotograph of the fabricated retina. The area of each pixel is $58\mu m \times 56\mu m$.

The fabricated retina has been extensively tested. In the following, we provide results of different experiments that we designed to investigate the performance of the retina under different conditions. Peak output event rate was 15*ns/event* (shorting Ack and Rqst). Power supply is 3.3V and current consumption depends linearly with output event rate (from 10µ*A* at zero output event rate to 3*mA* at 1.6*Meps* (eps = events per second)).

A. Calibration Experiments.

We have calibrated our retina under three different illumination conditions: darkness, ambient laboratory illumination, and bright illumination. The retina bias currents and voltages were kept the same in the three cases. In the three cases, we obtained a great improvement in the performance after doing calibration. Fig. 4 summarizes the performance of the retina before and after optimum calibration. In Fig. 4, the histograms of the pixels output frequencies under uniform illumination are represented. Each row in Fig. 4 corresponds to a different illumination condition. The left column represents the output frequencies before calibrating the retina, while the right column represents the pixels output frequencies after optimum calibration. We can observe that the performance of the retina is very similar for the ambient illumination and for the illumination under a bright light source. However, the mismatch is higher for low light. The reason is that in low light conditions the $\Delta I_{photo}/I_{photo}$ in equation (5) contains also the mismatch due to the photo diodes dark currents which become significative under this condition. When light shines on the retina, the I_{photo} denominator increases and the mismatch due to dark current becomes negligible. From our experiments, we have also verified that the retina performance is not severely degraded when the retina is calibrated under a given light condition and this illumination condition changes. However, the retina performance is severely degraded if the calibration was done with low light.

B. Contrast Extraction Experiments

Fig. 5 presents results of experiments where we presented to the retina an image composed of half black and half white/gray regions separated vertically. The relative contrast between the two regions varied from a 100% contrast (for half black and half white) to a 10%

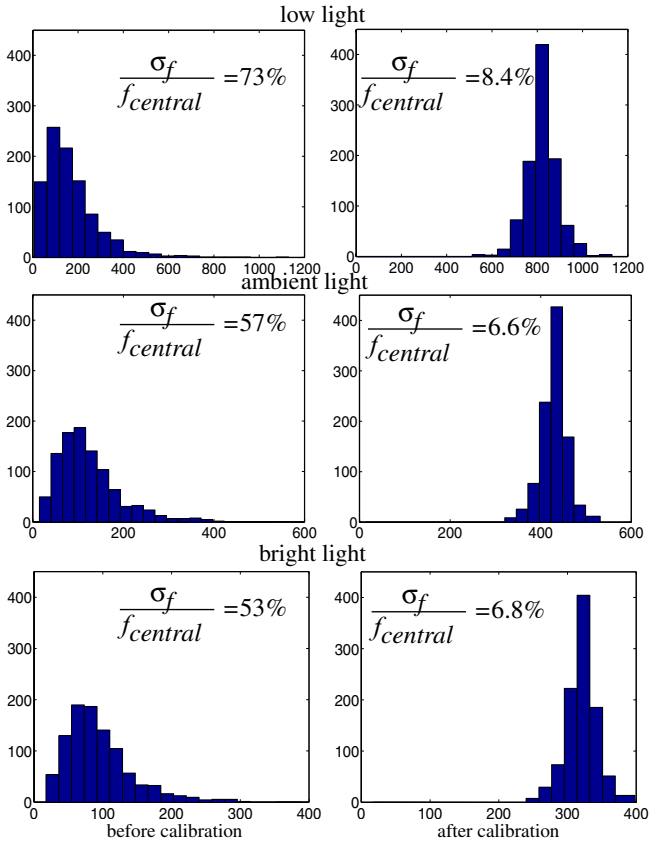

Fig. 4. Frequency histograms of the retina before and after calibration under different illumination conditions

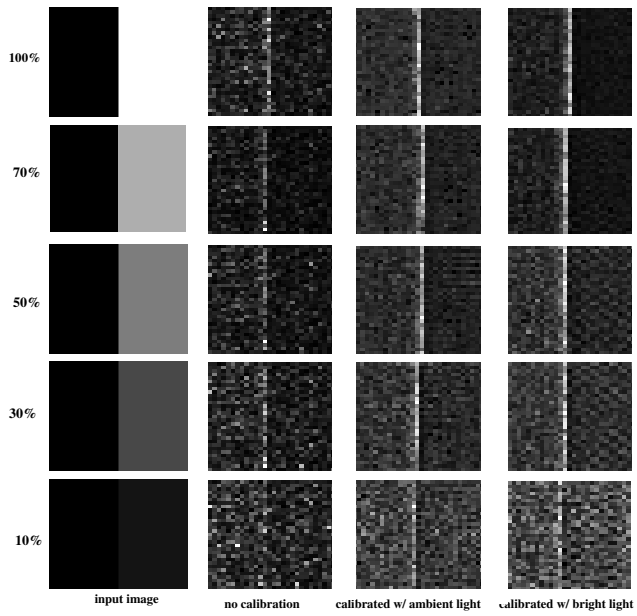

Fig. 5. Images acquired for different contrast levels

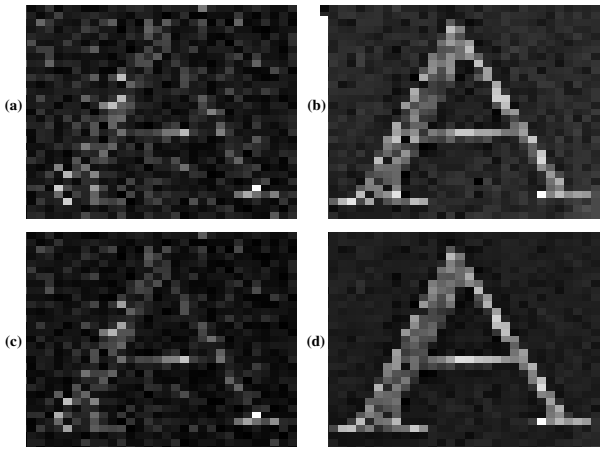

Fig. 6. Image acquisition under different illumination conditions

contrast (half black and half dark gray). The input images presented to the retina are plotted on the first column of Fig. 5. We captured the image with the retina calibrated with different calibration conditions: uncalibrated retina (second column in Fig. 5), retina with the optimum calibration weights and current I_u obtained for the ambient light conditions (third column), retina with the calibration weights and current I_u optimized for the illumination with a bright light source (last column in Fig. 5), so that in this last case the illumination conditions match the calibration conditions. As can be observed calibration not only reduces FPN but also allows to clearly recognize edges when low contrast images are presented to the retina. In the 10% contrast image, edge recognition is impossible with the uncalibrated retina. Observe also that resolution is not severely degraded when the illumination conditions do not match the calibration conditions.

C. Performance under different illuminations

To examine the retina performance under different illumination conditions, we acquired the same static input under different illumination conditions. These results are shown in Fig. 6. Fig. 6(a) and (b) were acquired under ambient illumination. Fig. 6(a) was acquired by the uncalibrated retina, while in Fig. 6(b) the retina was calibrated. The calibration used in Fig. 6(b) was also optimized for ambient illumination conditions. Fig. 6(c) and (d) were acquired under bright illumination. In Fig. 6(c), the retina was uncalibrated, and in Fig. 6(d) we were using the same calibration than for Fig. 6(b).

V. Conclusions

We have presented a contrast retina chip that provides its output as an AER stream. The contrast is computed as a result of multiplying and dividing currents at each pixel. This fact allows to calibrate mismatch by using one unique trimmable current per pixel. We provide descriptions of the design of the retina pixel and its calibration circuitry. We also provide experimental results illustrating the correct operation of the retina and how it benefits from its calibration capability.

VI. Acknowledgements

This work has been supported by spanish research grant TIC2003-08164-C03-01 (SAMANTA), and EU grant IST-2001-34124 (CAVIAR).

VII. References

[1] M. Sivilotti, *Wiring Considerations in Analog VLSI Systems with Application to Field-Programmable Networks*, Ph.D. Thesis, California Institute of Technology, Pasadena CA, 1991.

[2] J. Lazzaro, J Wawrzynek, M Mahowald, M Sivilotti, D. Gillespie, “Silicon Auditory Processors as Computer Peripherals,” *IEEE Transactions on Neural Networks,* vol. 4, No. 3, pp. 523-528, 1993.

[3] W. Maass and C. M. Bishop (Eds.), *Pulsed Neural Networks*, MIT Press, Boston MA, 1999.

[4] K.A. Boahen and A.G. Andreou, "A contrast sensitive silicon retina with reciprocal synapses, "*Advances in Neural Information Processing Systems* (NIPS 1991), Vol. 4, pp. 764-772, Morgan Kaufmann Publishers, San Mateo, 1992.

[5] J. E. Dowling, *The Retina: An Approachable Part of the Brain*, Harvard University Press, Cambridge MA, 1987.

[6] S. Grossberg, E. Mingolla, and J. Williamson, “Synthetic Aperture Radar Processing by a Multiple Scale Neural System for Boundary and Surface Representation,” *Neural Networks*, vol. 8, No. 7/8, pp. 1005-1028, 1995.

[7] B. Linares-Barranco and T. Serrano-Gotarredona , "On the Design and Characterization of Femtoampere Current-Mode Circuits," *IEEE Journal of Solid-State Circuits*, vol. 38, No. 8, pp. 1353-1363, August 2003.

[8] C. Mead, *Analog VLSI and Neural Systems*, Addison Wesley, Boston MA, 1989.

[9] E. Vittoz and X. Arreguit, “Linear Networks based on Transistors,” *Electronics Letters*, 29, pp. 297-299, February 1993.

[10] A. G. Andreou and K. Boahen, “Translinear Circuits in Subthreshold CMOS,” *Analog Integrated Circuits and Signal Processing*, Kluwer, no. 9, pp. 141–166, Apr. 1996.

[11] T. Serrano-Gotarredona and B. Linares-Barranco, "CMOS Mismatch Model valid from Weak to Strong Inversion", *Proc. of the 2003 European Solid State Circuits Conference,* (ESSCIRC’03), pp. 627-630, September 2003.

[12] B. Linares-Barranco, T. Serrano-Gotarredona, and R. Serrano-Gotarredona, "Compact Low-Power Calibration Mini-DACs for Neural Massive Arrays with Programmable Weights," *IEEE Trans. on Neural Networks*, vol. 14, No. 5, pp. 1207-1216, September 2003.